X-ray micro-CT investigation of metal recycling in egg-shaped crucibles during the Middle Iron Age

By

A. K. Bach

in partial fulfilment of the requirements for the degree of

Bachelor of Science
in Applied Earth Sciences

at the Delft University of Technology,

Supervisor: Dr. ir. D.J.M. Ngan-Tillard
2nd Supervisor: Dr. J.H.L. Voncken

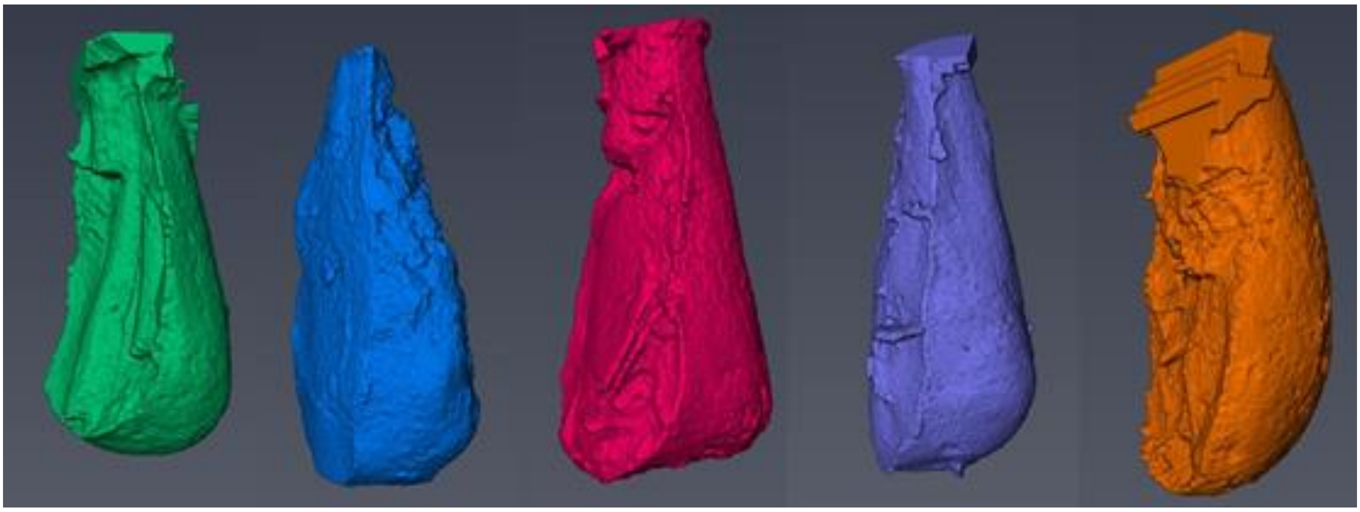

TU Delft

Abstract

During the extension of a sport complex near Tilburg, The Netherlands, some archeological objects were discovered. Some shreds of pottery seem to confirm that the objects found were originating from the Middle Iron Age.[1] Some of the objects were egg-shaped and hollow, with a small opening on the tip. The objects did awaken the thought that they might have been used as molds for melting metal. In this report the egg-shaped crucibles, or now called 'eggs' are further investigated.

The crucibles are examined by X-ray micro-CT scans and XRF analyses. The micro-CT scans are viewed and processed by Avizo 9.3. Results show that the eggs consist out of a half shell which is wrapped into a second shell. The second shell was still soft when wrapping, and therefore the metal scraps laid down inside the lower shell left some imprints within the outer shell. Also some highly attenuating materials can be found on the scans. This indicates the presence of metals as well as metal oxides or minerals with a high atomic number. In three eggs a large quantity of highly attenuating materials is found. In two of those eggs, these materials are seepage of metal that has been molten. In the other egg it is more likely to be a mineral, since the material is surrounding vesicles formed during the heating of the eggs. The XRF data showed that the objects are made out of clay. Some glassy looking parts on the outside of the eggs turned out to be precipitated quartz. The main metal that has been molten was found to be bronze, since high amounts of copper and tin were found.

Table of Content

Abstract 1
1 Introduction 4
2 Methodology 5
2.1 X-ray Micro-CT 5
2.2 XRF analysis 5
3 Data processing 6
4 Results 7
4.1 Image and data analysis of micro-CT scans 7
4.1.1 Features 7
4.1.2 Internal structures 7
4.1.3 Metal content 10
4.1.4 Egg cavities 12
4.1.5 External tool marks 13
4.1.6 Iron tool 15
5 XRF Analysis 16
6 Other analyses 18
7 Interpretation of the results 19
8 Conclusion 20
9 Recommendation 21
Bibliography 22
Appendix I: Micro-CT images of eggs 23
Appendix II: XRF Results 24

1 Introduction

Strange objects have been recovered from a Middle Iron Age fire pit excavated in Tilburg (Figure 1, left and middle) in 2016. They are made of baked clay and are egg-shaped and hollow (Figure 1, right). Their pointed end presents a small opening. Their thick wall consists of a half shell that is fully wrapped in a second shell. The outside of the outer shell is molten and bears marks of griping tools. XRF measurements on “egg” fragments indicated locally high metal contents. This led archaeologists to think that these objects have been used as lidded crucibles in some sort of metallurgical process. After a literature search[7], it appeared that similar crucibles have been recovered from prehistoric sites in Germany and France.

X-ray micro-CT scans of the objects can help archaeologists to better understand how these objects were manufactured and used. Probably, the most valuable results of the scans are the shapes that seem to be impressed into the roof of the cavities. These, also visible in some broken “eggs” (Figure 1, right image, top right object), are likely to be the metal scrap that was melted in these crucibles.

A series of 15 crucibles have been scanned for the Cultural Heritage Agency of the Netherlands. A rusted crust found at the same excavation has been scanned too. The scan of the crust uncovered a strange plier like tool made of folded metal sheets.

In a first stage, this thesis will aim at:

- visualising both the external and internal structure of the scanned crucibles
- elaborating a procedure to perform a morphometric analysis of the numerous features that the crucibles show
- exploring the use of the metal tool in the manufacture of the crucibles.

Results of the analysis of the digital objects will help to quantify the degree of standardisation of the crucible production, pinpoint at zones deserving further investigations (XRF, thin sections, and possibly SEM and EDEX), and categorize objects recycled in the crucibles during the Iron Age in terms of shape and size.

In a second stage, hand held XRF data acquired within the framework of this thesis at the Cultural Heritage Agency of the Netherlands will be exploited to find out:

- which metals were melt in the crucibles,
- further understand metal melting in the crucibles

The techniques used to acquire the micro-CT scans and the XRF data are described in chapter 2. Data processing is explained in chapter 3. Results are presented in chapter 4 and interpreted in chapter 5. The conclusion can be found in chapter 6 and recommendations in chapter 7.

Figure 1 Excavation of the fire pit (left and middle) where the egg-shaped crucibles (right) have been recovered. The fire pit was discovered during a construction project in Tilburg[1].

2 Methodology

The crucibles have been scanned using the X-ray micro-CT scanner of the faculty of Civil Engineering and Geosciences, a Nanotom manufactured by General Electric Sensing and Inspection Technologies/Phoenix X-ray, Wunstorff, Germany. The XRF analysis of the crucibles has been conducted with a handheld X-ray Fluorescence analyzer of the Cultural Heritage Agency of the Netherlands, a Niton XL3t apparatus.

2.1 X-ray Micro-CT

X-ray micro-CT (computed tomography) is a non-destructive technique that can be used to inspect the internal composition and structure of a wide range of materials, including archaeological remains. It is sketched in Figure 2 and described[2] as follows for desktop systems similar to the Nanotom. “In laboratory-based micro-CT scanners, a source of polychromatic X-rays illuminates the studied object, whilst a flat detector records the X-ray transmitted through the object. The object is rotated stepwise and at each step, a series of 2D radiographs is recorded. The scanning parameters (voltage and current of the X-ray beam, exposure time, number of radiographs per step and step angle) are selected to reach best compromise between spatial resolution, density contrast resolution and scan acquisition time. The radiographs are then processed with the help of reconstruction algorithms to derive patterns of variations in attenuation for 2D slices perpendicular to the axis of rotation that is used during radiograph acquisition. The reconstructed 2D slices have a finite thickness and consist of elementary building blocks called voxels. Each voxel has a specific grey value. The grey value is a measure of the linear X-ray attenuation coefficient of the materials present in that voxel. It depends on the local density and the chemical element(s) present in the voxel, together with the incident photon energy. The set of parallel 2D slices allows rendering and analysing the object in 3D.”

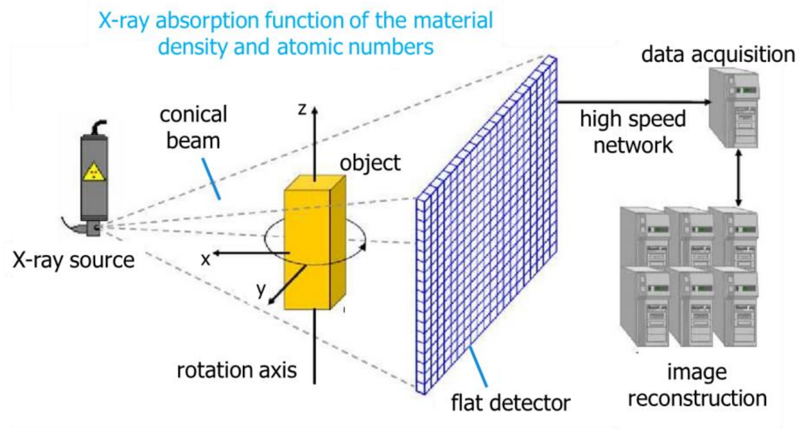

Figure 2 Schematisation of X-ray micro-CT data acquisition (Ngan-Tillard, pers. communication 2017)

The crucibles have been scanned with a voltage of 100-150 keV, an electric current of 170-220 µA and a voxel size of about 30 µm. For the large crucibles (crucibles Til5 and Til8), a multiscan, made of two scans has been recorded to achieve a voxel size of 30 µm. The objects have been reconstructed with the commercial software VG Max and the reconstructed objects have been analyzed using Avizo 9.3.
It should be noted that X-ray artefacts are inherent to desktop X-ray micro-CT and have to be identified to avoid an erroneous interpretation of the scans.[3]

2.2 XRF analysis

XRF or X-ray fluorescence is an analytical technique to determine the composition of elements present in an object using short-wavelength X-rays[4]. When an object is exposed to short-wavelength X-rays, ionization of the atoms of the object takes place. As a result of this ionization the atoms release energy in the form a photon. The emitted photon has a specific wavelength for each element and by determining the wavelength the element can be determined[4]. The hand-held XRF analyzer provides semi-quantitative results for certain elements only. For example, it cannot detect light elements, such as oxygen and sodium.
Each XRF scan was done at a specifically chosen location on the crucibles. In total 29 XRF scans were performed.

3 Data processing

For the processing of the micro-CT scans, Avizo 9.3 has been used. Avizo is a powerful commercial program that allows 3D visualization and analysis of micro-CT scans. The set of 2D images produced by the reconstruction program VG Max can be loaded directly into Avizo. Some functions of Avizo are often used and are briefly explained below following.[5,6]

The interior of the 3D data set can be viewed in real time (from any position) using an intuitive technique called volume rendering. This technique simulates light transmission through the object from the viewing point, making the voxels more or- less semi-transparent, so that they do not obstruct the view of the voxels placed behind them. By choosing a low transparency, the exterior of 3D object can be displayed. By increasing the transparency, inner components like metal residues contained in the egg shells can be visualized. The reconstructed object can be intersected by multiple cross-sections. Orthoslices are cross-sections that are parallel or perpendicular to the set of 2D images produced by the reconstruction algorithm. By adjusting their number, one can scroll through the whole object. Slices are cross-sections with an arbitrary orientation. Cross-sections can be used to clip the 3D volume in order to inspect its inside. Subsequently, images can be segmented into diverse components to allow a quantitative analysis of each component (Label Analysis). Materials or features that are distinct because of their attenuation– like baked clay, metal residues, cavities, and other components of the crucibles…) can be identified, separated using segmentation tools, and counted before being visualized and subjected to digital size, shape, and orientation analysis using the function Label Analysis. Most used shape parameters are Volume3D, Area3D, 3D feret dimensions (3DLength, 3DWidth and 3DBreadth), orientation of maximum feret (Orientationphi, Orientationtheta), principal moments of inertia and their associated eigenvectors. Other shape parameters like shape_VA3D, Elongation, Flatness, and Anisotropy can be calculated using the principal moment of inertia to characterize the shape of the object. The shape_VA3D calculates the spherity of an object; it takes a value of 1 for a perfect sphere. The Elongation is the ratio between the medium and largest principal moments of inertia. The Flatness is the ratio between smallest and medium principal moments of inertia. The Anisotropy is 1 minus the ratio of the smallest and largest principal moments of inertia. The more equal the values for the dimensions are, the more equal the shapes of the objects are.

Segmentation requires image thresholding, in other words, image conversion based on grey levels into binary images in order to select the phase of interest, for example, for the crucibles, baked clay, metal inclusions, vesicles, egg cavity, etc. Interactive Thresholding is one of the many possibilities offered by Avizo to threshold images. When objects touch each other, one can use a sequence of Erosion, Filtering by Volume and Dilation to separate the objects. The surface of the separated objects can be generated and converted into a stl file that can be sent to a 3D printer to obtain of physical replica of the object. The function Fill Holes can be used to close inner porosity so that only the outer surface of the object is produced.

4 Results

4.1 Image and data analysis of micro-CT scans

Micro-CT images of the eggs, made with Avizo can be found in Appendix I.

4.1.1 Features

First the basic information on the shape of the eggs was extracted with Avizo using the function Label Analysis (Table 1). Information provided in Table 1 for Til5 is not complete. When the egg was scanned, the egg was filled with some sand. As the sand was found to be difficult to separate from the egg itself, the 3D Volume and Area of Til5 could not be calculated.

The volume of the eggs was calculated before and after applying the Fill Holes function so that porosity could be retrieved. Note that all pores connected to the outside are not filled with the Fill Holes function. Nevertheless, the calculation leads to a reasonably good estimation of the total volume of the egg (baked clay including vesicles). According to Table 1, the maximum porosity is 4.9%, therefore it can be said that the porosity of the eggs is low. The Area 3D function calculates the area of both the external and inside surfaces of the egg as well as the area of holes and cracks contained in the egg. The Area 3D function was used after the function Fill Holes was applied and lead to the values listed in the ”Area filled” column. Since the holes were filled, only the area of voids connected to the outside of the egg is included in the value of “Area filled”, which leads to a slight overestimation of the eggs Area.

Table 1 morphometric parameters and porosity of the crucibles

Egg	Width (mm)	Breadth (mm)	Length (mm)	Volume (mm^3)	Volume filled (mm^3)	Porosity (%)	Area filled (mm^3)
Til1	46.3	56.6	73.1	74465.4	77533	4.0	21161.8
Til2	49.4	60.8	76.8	92887.8	94254	1.4	35236.8
Til3	51.9	65.4	81.9	80820	83057.3	2.7	40682.7
Til4	51.8	61.9	63.9	64235.5	66921.3	4.0	30303.4
Til5	55.0	64.7	89.4				
Til6	49.4	57.5	73.5	85996.2	88522.4	2.9	27327.2
Til7	45.3	51.1	70.6	50931.4	53575.8	4.9	16286.7
Til8	51.0	68.6	84.0	93619.6	95090.9	1.5	38757.4
Til9	51.5	59.0	73.2	78739.2	80321.5	2.0	26657.2
Til11A	25.2	44.3	68.5	21345.1	21666.8	1.5	10379
Til12	47.0	61.6	80.6	62025.5	63544.6	2.4	33186.5
Til13B	27.3	44.7	50.5	17320.4	18005.9	3.8	21981.2

4.1.2 Internal structures

The micro-CT scans highlight well the inner structure of the eggs even if the egg half shell and wrapping layer can only be separated digitally when a crack runs along their interface (Figure 3). The baked clay contains vesicles of various sizes that are unevenly distributed. Moreover its solid part presents some differences in density or chemical content since it shows up on the scans in various shades of grey.

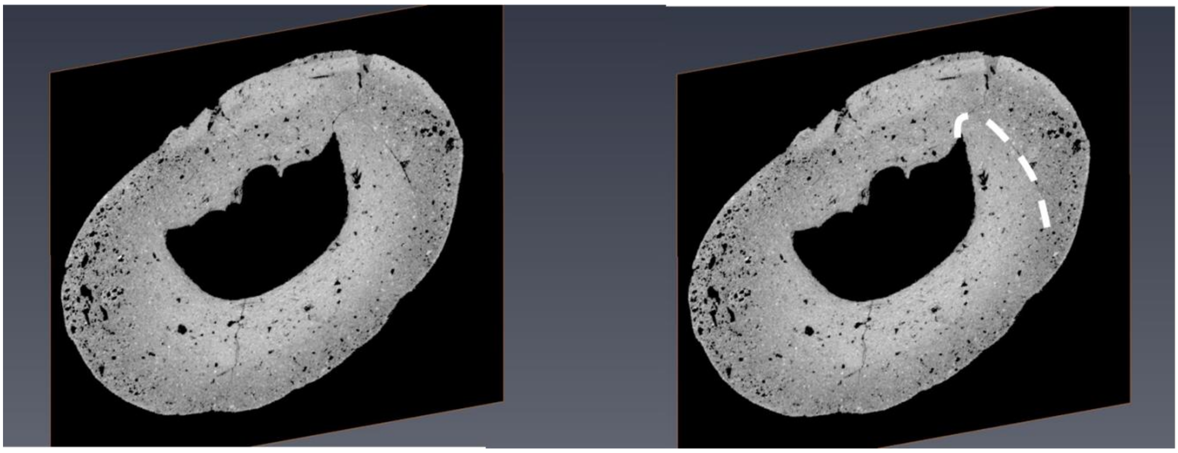

Figure 3 Orthoslice showing the inner structure of Til1. The crack highlighted with the dashed line outlines the separation between the half shell and the wrapping layer.

The metal scrap that had to be molten was laid in the half shell and was wrapped in a second shell before the egg was placed vertically in the fire pit. While the half shell was already dry when objects were laid down, the second shell was wet and soft so that it could be wrapped tightly around the half shell and the metal scrap. As a result, the metal scrap left its imprint on the inside of the wrapping layer. In figure 4 an image showing the imprints in Til1 and Til4 and their dimensions can be found. Dimensions should help archaeologists in their identification work.
A negative of the imprints can be produced digitally to reconstruct the objects that have been melted (Figure 5 to Figure 8). Void is "thresholded" to represent the cavity displayed and cropped to eliminate outside void as well as some cracks in the egg.

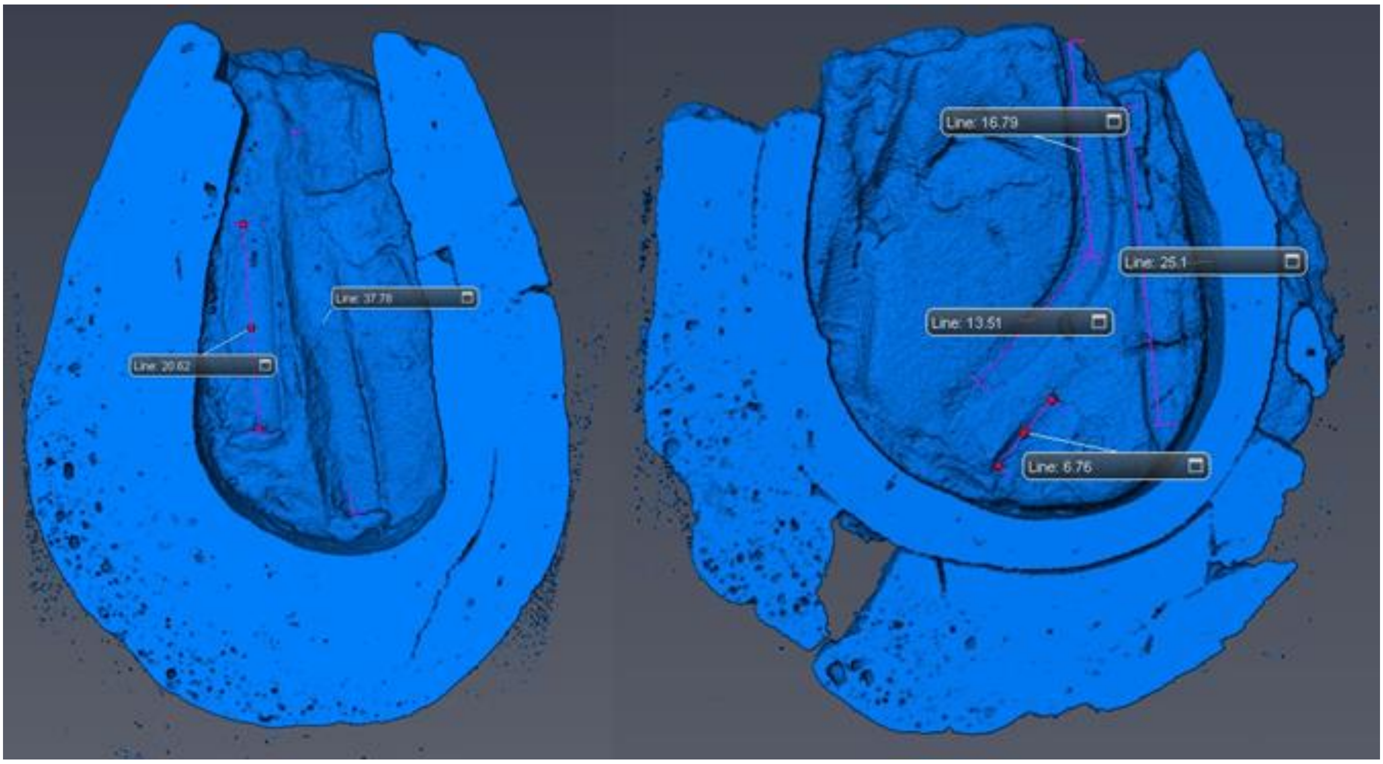

Figure 4 Imprints and their dimensions in Til1 and Til4

Some of the imprints have been identified5. They are straight metal bars, filaments (Figure 5), fibulas (Figure 6), folded metal plates (Figure 7), and twisted threads. Others are still an enigma (Figure 7 and Figure 8).

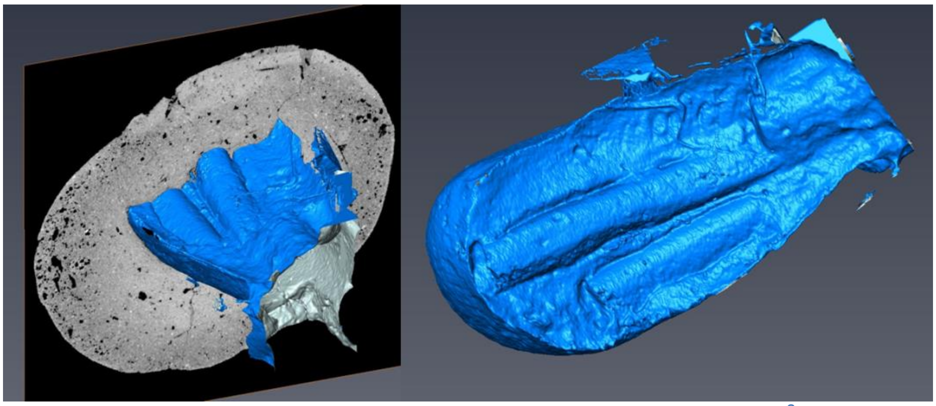

Figure 5 Negative of imprints left by two long bars and thin filaments with a 90^{o} twist in the cavity roof of Til1. The negative is represented by generating the surface of the thresholded egg cavity.

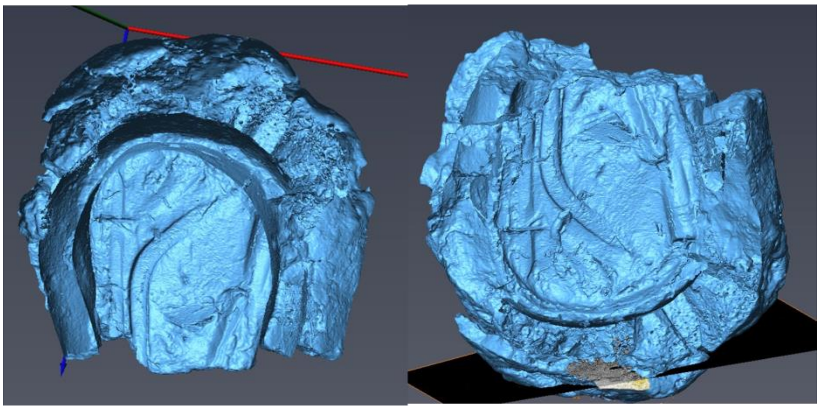

Figure 6 Imprints (left) and negative of imprints (right) in the cavity roof of Til4. A fibula is clearly visible in the cavity lid. Note the small hook that pierced the cavity (right picture) and would only be visible as a hole on the roof cavity (left picture) without a micro-CT scan.

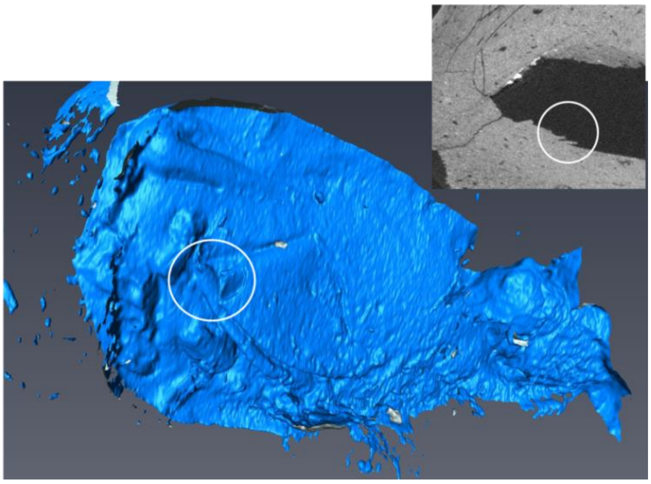

Figure 7 Negative of Imprints in the cavity roof of Til6. A circular metal sheet folded into two twice can be seen. The torn corner gives the impression that the disk was made of 2 sheets. Note also the non-identified object with a rounded end on the top left corner of the blue surface.

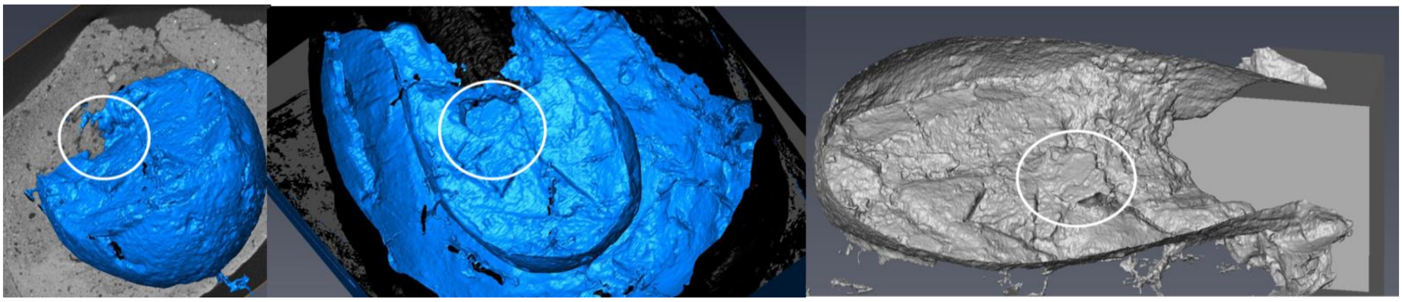

Figure 8 From left to right. Cavity surface of Til9 intersected by a cross-section showing the complex geometry of the egg lid; negative of imprints and imprints. The ring like item with two small spikes highlighted by the circle results from clay intrusion.

4.1.3 Metal content

Material that attenuates highly X-ray shows up as white on the grey micro-CT scans (Figure 9) and can be separated from the eggs using Interactive Thresholding. Highly attenuating material consists of either metal, metal oxide or mineral containing chemical elements with a high atomic number that have been possibly produced during the heating of the (organic) clay.

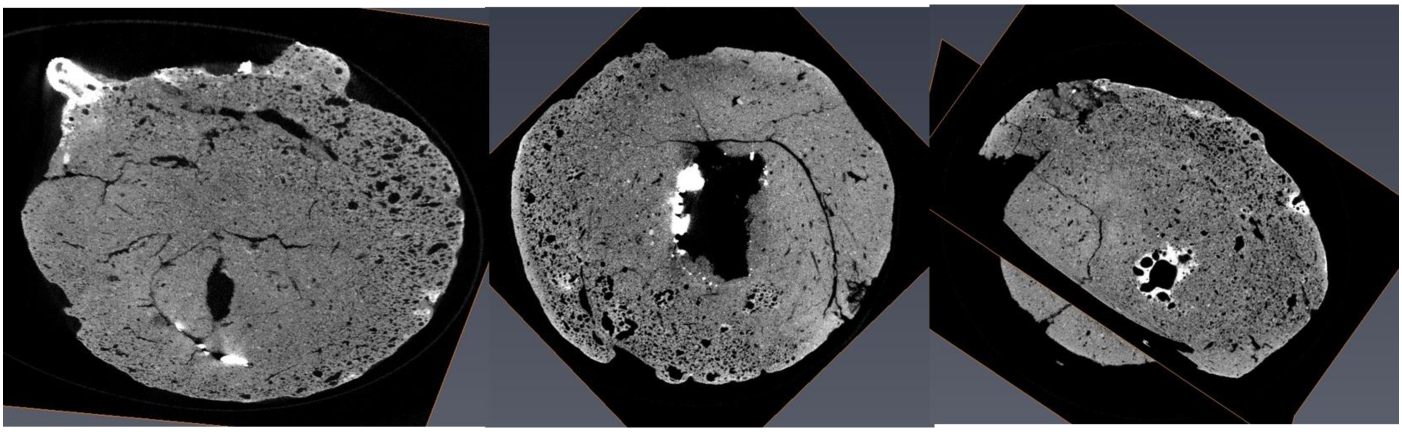

Figure 9 Examples of highly attenuating features in Til6, Til3 and Til12 including large protrusion at the base of Til6, metal seepage in Til6 and Til3, metal residue in Til3, and material surrounding vesicles in Til12.

The Interactive Thresholding function was adjusted by trial and error to model the highly attenuating material. First the maximum threshold value was set to the maximum grey values contained in the data set and the minimum threshold value was decreased until noise started to appear on the "thresholded" image. This allowed filtering out small objects that cannot be easily identified.

Almost every egg contains some amount of highly attenuating material, but most of it was found on the external surface of the eggs. It cannot be sure that this material belongs to the eggs themselves and does not originate from the egg surroundings. Three eggs (Til3, Til6 and Til9) do contain a noticeable amount of highly attenuating material inside their shells or inner cavity. In the following sections this material is further discussed.

4.1.3.1 Til3

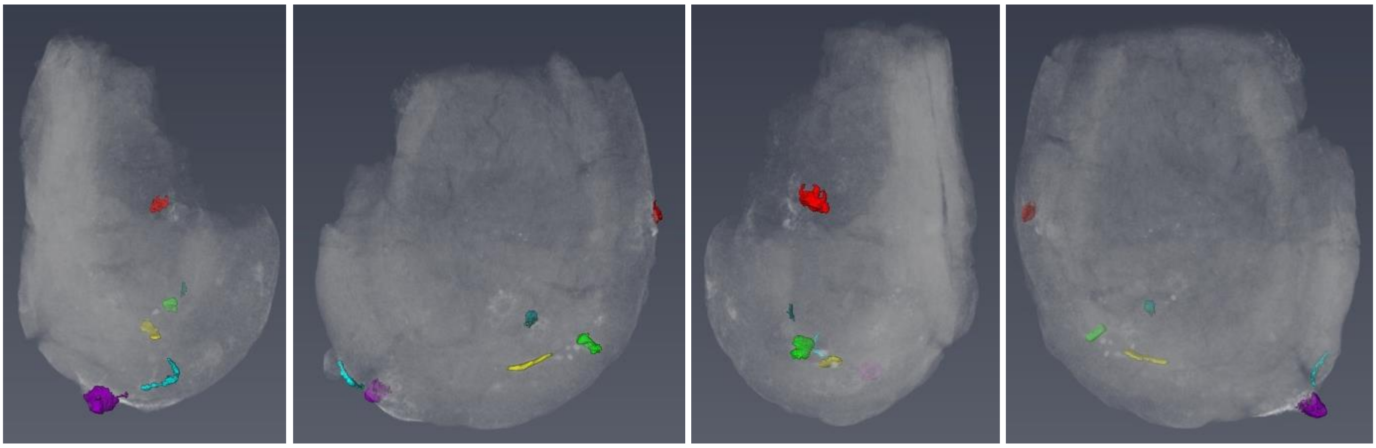

Figure 10 Front view of Til3, including turns of 90, 180, 270 degrees

Figure 11 Metal content inside Til3

Figure 10 shows where the highly attenuating inclusions are situated in Til3.

The front view of the egg and views after 90, 180 and 270 degrees turns are displayed. Only volumes greater than 1 mm^3 are taken into consideration. The red, blue and purple volumes are located on the external surface of the egg. The other three volumes are located inside the egg. Figure 11 shows the precise position of these three volumes. The yellow and green volumes seem to result from metal seepage from the egg cavity to the interface between the half shell and the wrapping layer via a crack network. In Table 2 the values for the volumes of the inclusions can be found. The following Interactive Thresholding values were used to model the large highly attenuating inclusions: 12052 – 12398.

Table 2 Metal volumes in Til3

Volume color	Metal volume (mm^3)
Purple	21.0
Green	16.9
Yellow	14.7
Red	6.6
Blue	4.6
Turquoise Blue	1.9

4.1.3.2 Til6

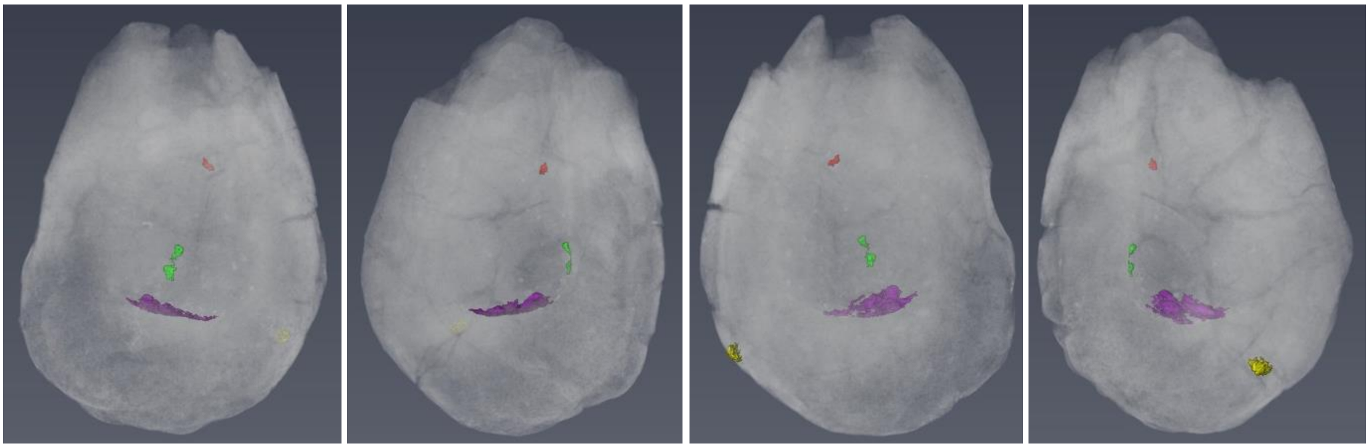

Figure 12 Front view of Til6, including turns of 90, 180 and, 270 degrees

Figure 14 Positions of metal content inside Til6. The egg has been clipped by a vertical orthoslice.

The same type of illustrations as for Til3 is shown for Til6 in Figure 12 to Figure 13. The following Interactive Thresholding values were used to model the large highly attenuating inclusions: 14640 – 15370. Only the yellow volume is situated on the outer surface of the egg. The purple volume is obviously a very large metal residue (Table 3) that has solidified at the bottom of the egg cavity while the egg was in a vertical position. The red and green volumes are probably metal residues too but they are much smaller (Table 3).

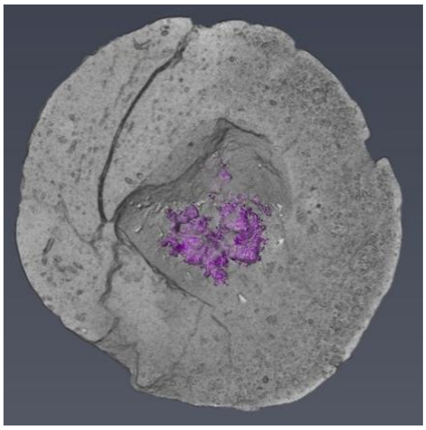

Figure 13 Large residue in Til6 viewed from above. The egg has been clipped by a horizontal orthoslice.

Table 3 Metal volumes Til6

Volume color	Metal volume (mm^3)
Purple	53.7
Green	3.4
Yellow	2.7
Red	1.5

4.1.3.3 Til9

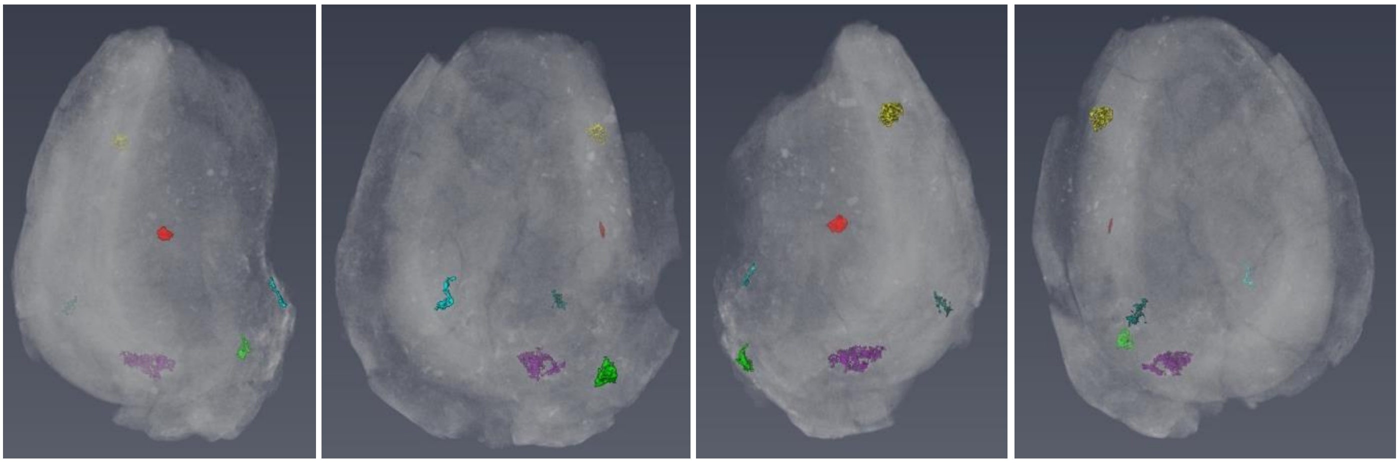

Figure 15 Front view of Til9, including turns of 90, 180, 270 degrees

Figure 15 displays the volumes of highly attenuating material contained in Til9. Six volumes greater than 1 mm^3 have been identified (Table 4). The purple and red volumes are inside the egg, the blue and green volumes are on the outside of the egg and the turquoise blue and yellow volume cannot be easily located. The turquoise blue and yellow volume are visibly part of the inside of the egg but are situated near the edge of the egg. Til9 is special because it contains large vesicles inside its shells that are fringed by highly attenuating volumes of complex shape (Figure 16). The left picture shows the large vesicle and the right picture the highly attenuating material that surrounds the vesicle. This is not only for the volumes shown in the above pictures, also smaller bubbles are also surrounded by highly attenuating volumes, but these volumes are smaller than 1 mm^3. In this case the volumes could be very rich in calcium ions that attenuate X-ray more than many of the other ions contained in clays. It is more likely that these volumes represent a mineral rather a metal. The following Interactive Thresholding values were used to model the large highly attenuating inclusions: 16053 – 17625.

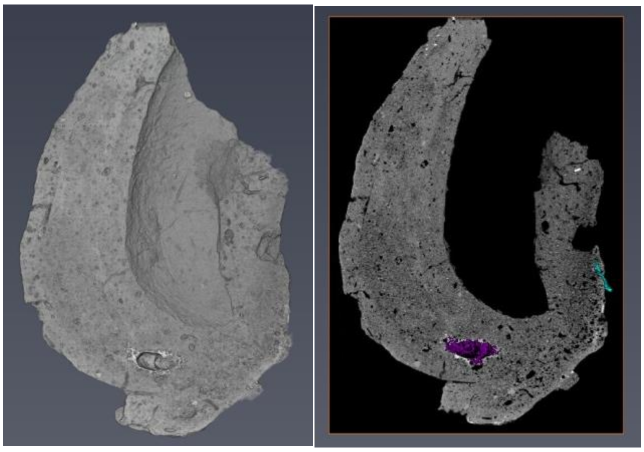

Figure 16 Bubble surrounded by volumes of highly attenuating material

Table 4 Metal volumes in Til9

Volume color	Metal volume (mm^3)
Purple	13.1
Green	5.5
Yellow	4.4
Red	1.9
Blue	1.6
Turquoise Blue	1.6

4.1.4 Egg cavities

The shape parameters of the egg cavities have been calculated for the eggs that are almost complete.
The function NOT, which turns voids into solid and solid into voids, was applied to the thresholded egg inside a Region Of Interest (ROI) box containing the egg cavity. The ROI box was adjusted before cropping the volume. With NOT, everything that is not part of the egg was turned into solid. The volume was then eroded to separate the cavity from cracks linked to the cavity. After erosion, the disconnected cracks were filtered out based on their volume. Then, the remaining volume was dilated to recover the size of the cavity. Cracks that were still linked to the egg cavity and air connected to the neck of the cavity were cut off iteratively as closely as possible with the Volume Edit function. The Volume Edit function was used without rotating the object to avoid re-sampling that would smoothen of density contrasts. This processing was clearly more time consuming than the processing used to visualize the

negative of the metal imprints. However, as it included a sequence of Erosion/Filtering and Dilation, it might have deleted fine details on the imprints.

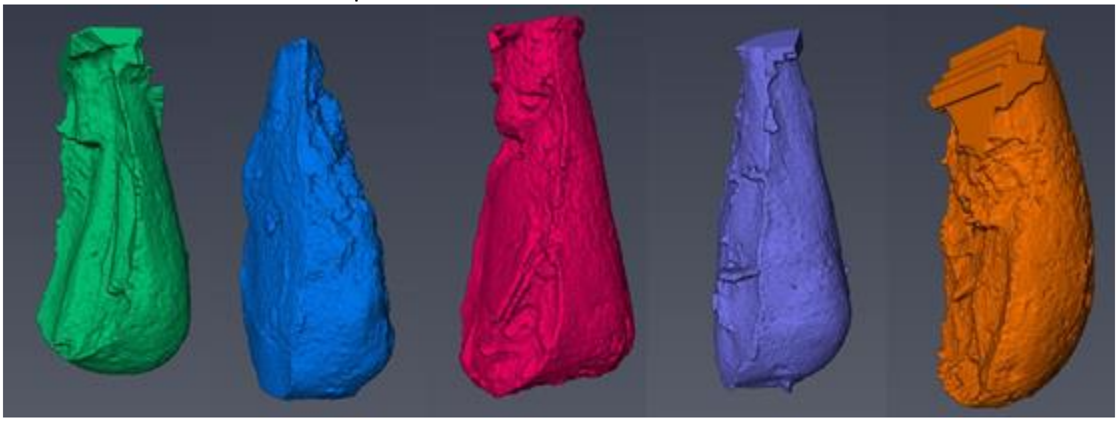

Figure 17 Cavity of eggs Til1, Til2, Til6, Til8 and Til9

Table 5 shows the 3D breadth, length, width, area and volume of the different cavities. It also presents shape parameters like shape_VA3D, Elongation, Flatness, and Anisotropy. These dimensions are shown to compare the shapes of the cavity.

Table 5 morphometric cavity parameters

Color	Egg	Breadth (mm)	Length (mm)	Width (mm)	Area (mm^2)	Volume (mm^3)	Shape_VA3D	Elongation	Flatness	Anisotropy
Green	Til1	26.4	54.1	22.3	3696.7	11019.2	3.68	0.16	0.51	0.92
Blue	Til2	29.6	57.9	22.2	4020.9	14454.8	2.75	0.23	0.48	0.89
Pink	Til6	27.9	52.1	25.4	3903.7	11375.7	4.07	0.21	0.65	0.86
Purple	Til8	32.6	62.1	24.2	4640.7	17348.3	2.94	0.17	0.75	0.87
Orange	Til9	30.0	51.3	25.2	4019.9	13771.9	3.03	0.25	0.46	0.89

Based on Table 5, it can be said that Til2 and Til9 cavities are most similar in shape, despite the fact that the bottom of Til2 cavity is straighter than that of Til9 cavity. The volume of the different cavities indicates the maximum volume of metal which could have been molten per egg. The Breadth, Length and Width indicate the maximum size of objects that could fit inside the cavities. It could be that some metal objects like the metal sheets were folded to fit inside the cavity.

4.1.5 External tool marks

The external surfaces of several eggs show marks that are thought to be left by a gripping tool (Figure 18). The marks have been measured and their dimensions are roughly the same (Figure 19). This in an indication that the same gripping has been used.

Figure 18 External marks of gripping tools on the external surface of Til1, Til2 and Til6.

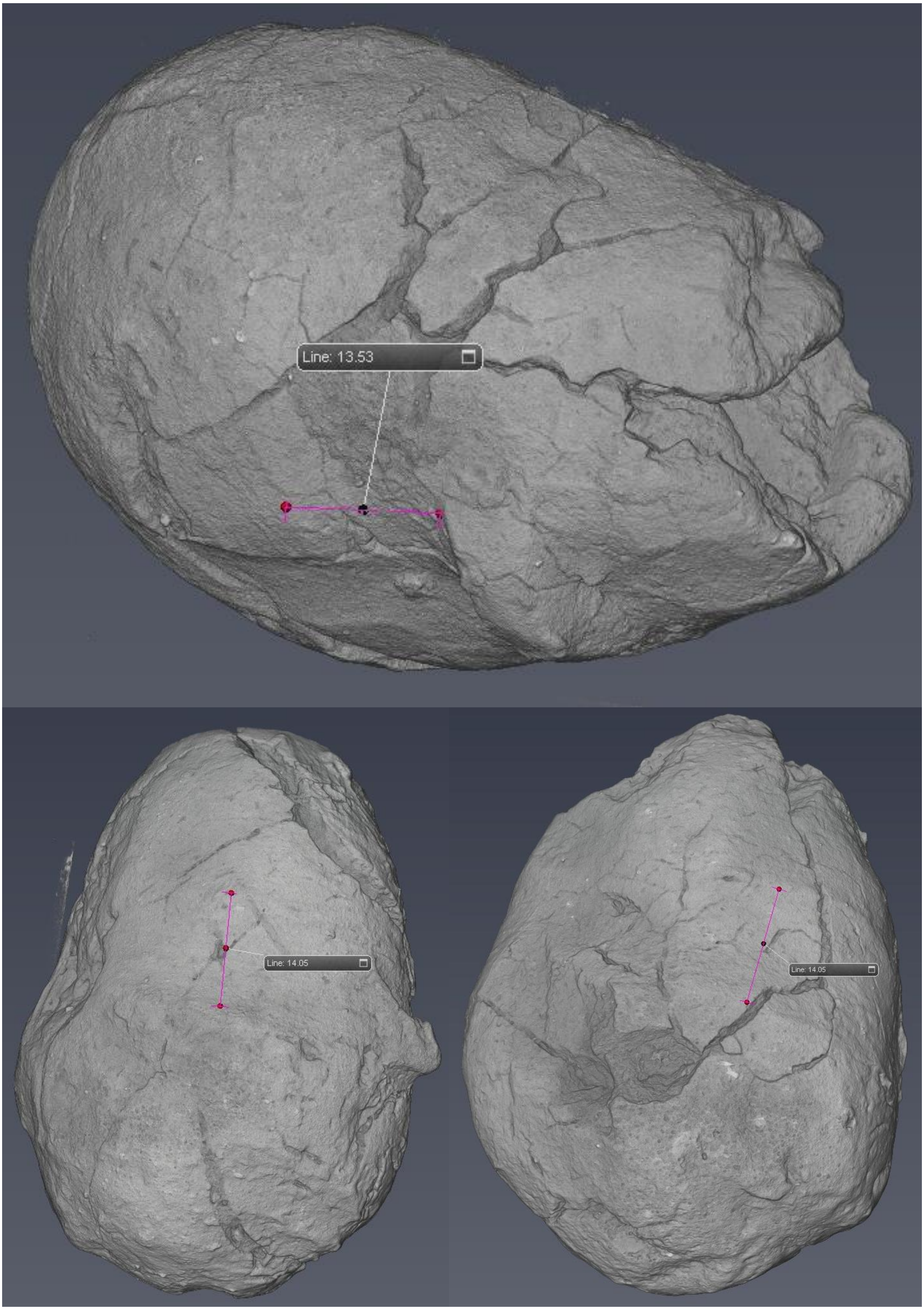

Figure 19 Dimensions of griptool marks (top: Til1, left bottom: Til2, right bottom: Til6)

4.1.6 Iron tool

Together with the eggs, an iron crust was found (Figure 20). First thoughts were that this was used to manufacture the eggs. Some scenarios have been worked out. First it was looked whether the iron crust was used as the grip tool mentioned above. But the eggs are too big to have been grabbed by the tool. The second scenario was that the tool was used as a mould to shape the half shell. But the cavities of the half shells are too wide to fit within the tool. A third scenario was that the tool was used as a formwork to shape the half shells. But the half shells are too short to have been moulded around the tool. Therefore it is not known what the iron tool was used for.

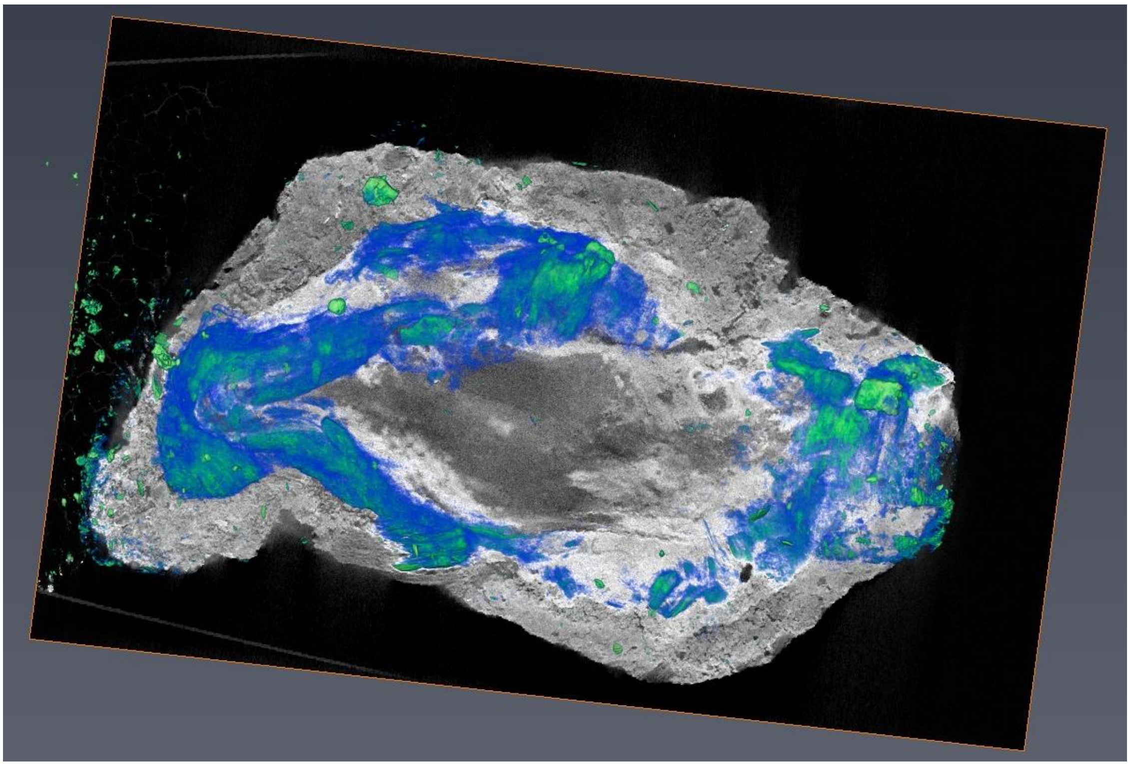

Figure 20 Iron crust with high attenuating parts in blue/green.

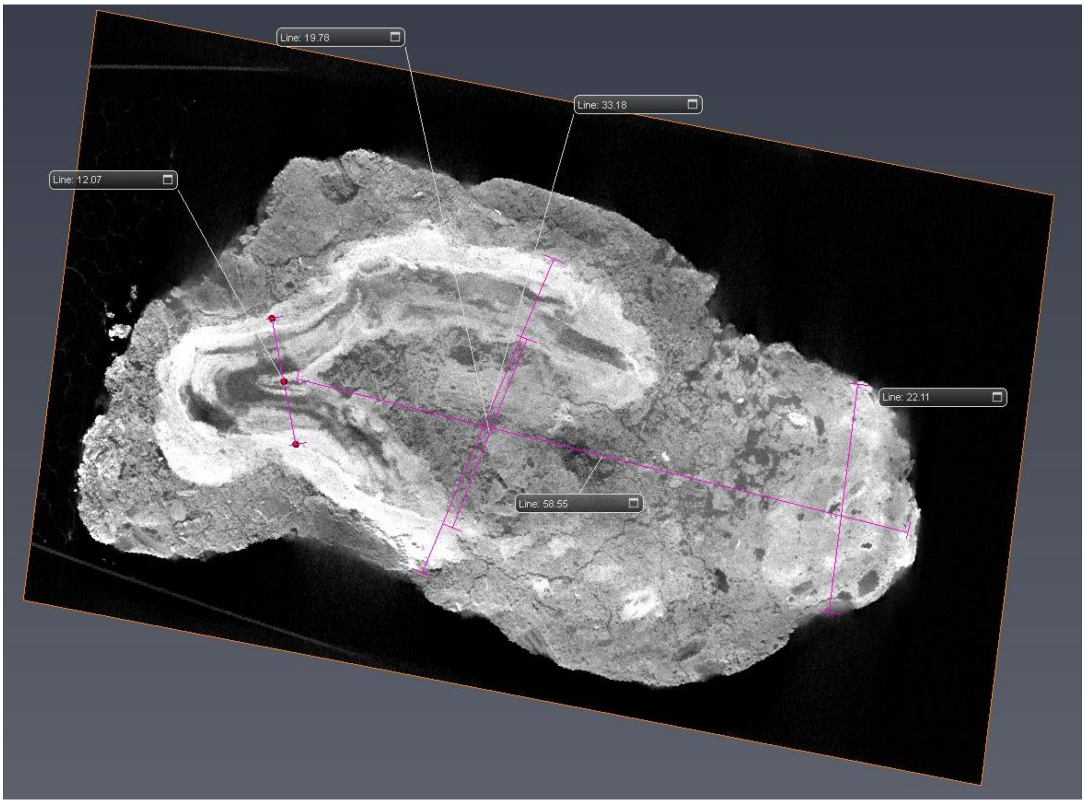

Figure 21 Iron crust with measurements

5 XRF Analysis

The results of the XRF analysis can be found in Appendix II. They have been produced by Bertil van Os of the Cultural Heritage Agency of the Netherlands in Amersfoort[7]. All eggs that exhibit interesting spots on their external surface were scanned. In total 29 XRF scans were done on the eggs. The scans were recorded with a handheld XRF machine, which provides semi-quantitative results for certain elements only. For example, as already mentioned above, it cannot detect light elements, such as oxygen and sodium. In the column Bal in Appendix 2, all elements that cannot be detected are summed. All pink crossed numbers are values that are around the detection limit and are therefore not accurate. They have been obtained for elements which are present in the eggs, but in really small amounts. The main elements can exist as oxides which percentages per total weight have been calculated. The ppm has been calculated for the minor elements.

Fe_2O_3, or hematite appears in large amounts in the processed data only for the scans which were targeting black looking spots. The amounts of Nickel and Cobalt are higher in average in these spots but still under the detection limit and therefore measured concentrations are not reliable. Hematite can be having various colors ranging from red to brown and black. It leaves a red trace when scratched against a rough surface. Another mineral consisting of iron and oxygen is magnetite. Magnetite is black, but magnetic as well. Since the spots on the eggs do not show any magnetism, it cannot be said the black spots are magnetite instead of hematite. It is also possible that contrary to what has been assumed in the quantitative analysis of the measurements, Fe is not present as component of an oxide and but in a piece of iron. The spots with the black looking spots were only located on the outside of the eggs. A good example is the big protrusion in figure 10, left, which has scan number 769.

The eggs are made out of clay. Clay is often rich in Si, Al, K, Ca and Fe and could also contain traces of Rb, Sr and Nb. All the other elements found in the XRF analysis are originating from the molten metal, the fuel used to heat up the small crucibles or the environment surrounding the eggs. Cu, Pb and Sn are not originating from clay or fuel and therefore it can be concluded that these are likely to be from the metals which were molten in the eggs.

From the XRF results it can also be seen that the 'glassy' looking spots on the eggs have another composition than the eggs. It can be assumed that the glassy looking spots are not originating from the eggs, but from the manure in which the eggs could have been packed, for an evenly distributed temperature and reduced environment[7]. Manure is rich in Ca, K and P. When manure is heated, the organic matter is burned and Ca, K and P remain. These elements are reducing the melting point of quartz, originating from the clay, and therefore quartz melts. When the temperature decreases, the glass, which is molten quartz with some dissolved imperfections, attaches to the outside of the eggs.

Correlations between the oxides are examined via the plots of Figure 22. The units for the plots are percentages for the oxides and mg/kg for the other elements. The diagrams show a linear correlation between Ca and K, which means that Ca and K are most likely originating from the same source. Rb and Sr are originating from the same source too since both are linearly correlated with K and Ca.

The (weak) negative correlation between Al and K indicates that Al and K are not originating from the same source. Since Al originates from the clay of the eggs, K does not and arises probably from the manure.

It is most likely that the metal that was molten was bronze, since copper and tin are present in the eggs. In egg Til11A the value for Pb is very high, which indicates that some lead has been molten. In the eggs Til2 and Til13B high amounts of Zinc are present, indicating that brass probably has been molten.

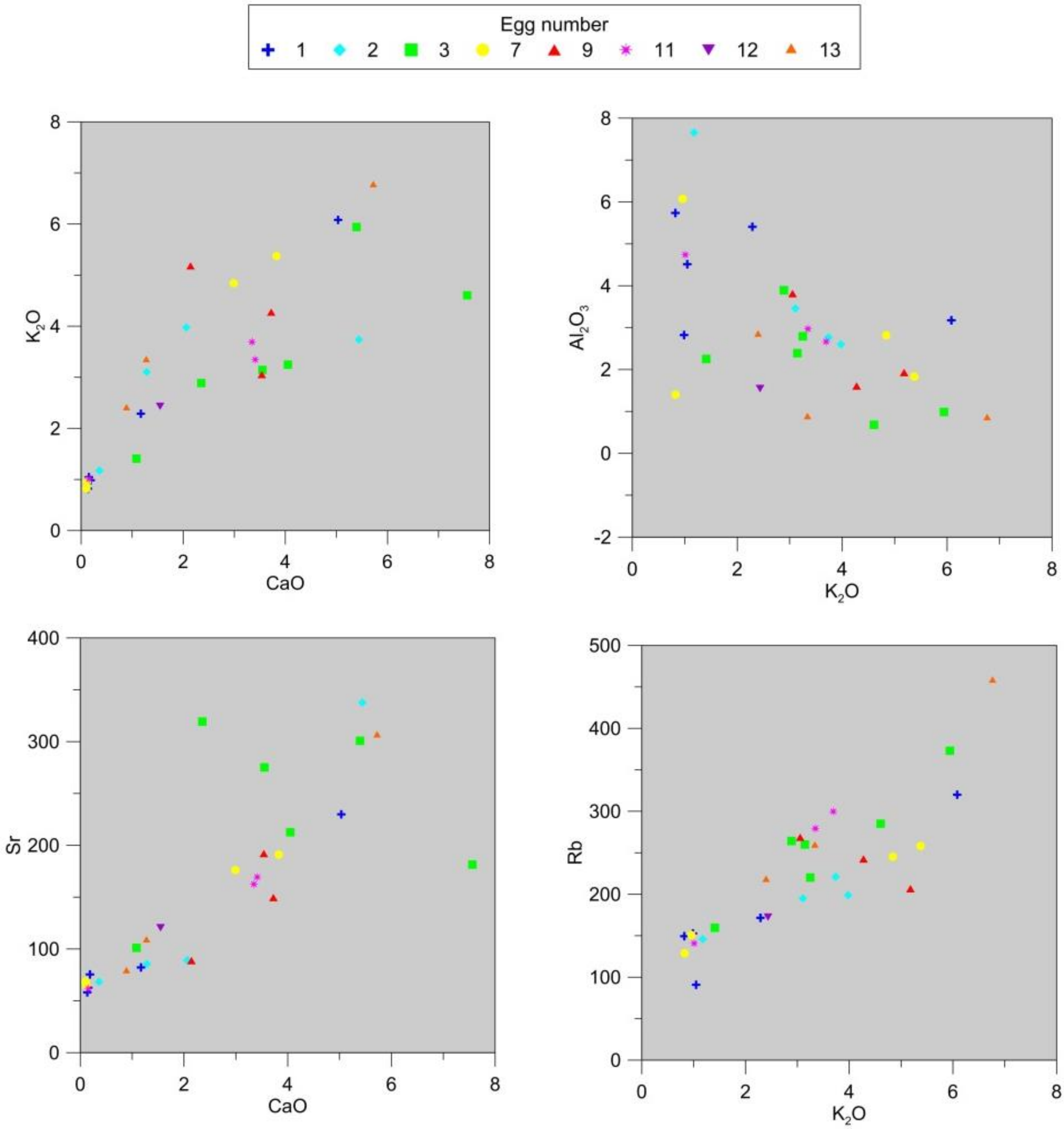

Figure 22 Correlation between oxides and chemical elements identified by the XRF analysis

6 Other analyses

The metal residue uncovered inside the cavity of Til6 has been imaged using an endoscope. It shows up on the images recorded with the endoscope as white spots similar to those observed on the external surface of Til13B, identified as bronze using the handheld XRF measurements.

7 Interpretation of the results

The egg-shaped crucibles found in a fire pit at a construction site in Tilburg were most likely used to melt metal scrap. First the inner half shells were formed from clay and were dried. The half shells were probably made manually. The iron tool discovered in a rusted crust recovered at the excavation site and first thought to have been used as formwork to shape the half shells fits tightly in only a couple of egg cavities. The metal scrap was placed in the half shell and wrapped into a second shell of soft clay to form an egg-shaped crucible. The imprints left by the metal scrap in the fresh clay lid have revealed that the crucibles were used to melt a variety of objects ranging from straight metal bars, filaments, twisted threads, to fibulas and folded metal sheets and many other small objects that have not been identified. It is possible that the metal sheets were folded to fit the 29 mm (in average) wide half shell.

Small size crucibles were fabricated most likely to optimize thermodynamic conditions for a homogeneous melt. The average of the volume of the cavity of the eggs is about 13000 mm^3, i.e., 13 mL of liquid metal could have been produced and this, provided the cavity would have been totally filled up with scrap. The eggs were possibly packed into manure before being laid vertically in the fire pit. The manure ensured an even temperature distribution and provided a reducing environment. The heating of the manure resulted in the formation of a glassy coating on the outside of the eggs[5,7]. The eggs were heated until the metal inside molten. During the heating, the half shell and the wrapping layer were heated too and baked. The (organic) clay used to make the eggs sustained mineralogical changes under the effect of heat. Glass and vesicles of various sizes and shapes were formed unevenly in the egg and phantoms of plant stems can be observed. By identifying the minerals present in the eggs and especially around the vesicles that are visible on the micro-CT scans, one could estimate the maximum temperature to which the eggs were subjected for melting the metal scraps[8]. After melting, the liquid metal was poured out of the egg. The XRF results on the cavity of fragmented crucibles show that the metal scarp that was molten was mainly bronze. In some of the eggs, there are also indications for the melting of brass and lead. The egg was grabbed with a plier that left traces on the egg surface to be placed in or removed from the fire pit. The iron tool in the rusted crust could not have been used for this purpose. Its opening is too small. The eggs were not always fully emptied. Some metal residue has been observed at the bottom of the cavity of one egg and traces of metal seepage have been found in between the shells of another egg.

8 Conclusion

The main objective of this thesis was determining the internal structure of the crucibles and the composition of the crucibles. With the help of Avizo, it was seen that the crucibles consisted of an inner half shell consisting of baked clay. The inner shell was wrapped in an outer shell, in which the metal scrap is packed. On the inside of the outer shell, some imprints of the metal scrap can be found. Some of these imprints have already been identified for example as fibula or folded metal disks, other imprints have yet to be identified.

The crucibles itself consists of baked clay. Some of the crucibles have some 'glassy' looking spots on the outside, which appears to be solidified quartz.

The second objective was to analyze the XRF data in order to determine the presence of metal residue and the metal elements present in the metal residue and in the crucibles as well. The XRF data show that the metal elements present are mainly copper and tin, which are the components of bronze. Also zinc and lead are present, where the zinc and copper form brass. Also some metal residues were collected inside the crucibles. The residue volumes vary in size and only a few large residues are found. The residue found in egg Til5 have been viewed with a low resolution endoscope and seem to have the same white color as the spots on egg Til13B, which also indicated bronze.

The third objective was to characterize the shape and size of the cavity of the crucibles. The cavity of 5 crucibles has been created, since these crucibles were almost intact. The cavity of the crucibles has an average volume of 13000 mm^3. They vary much in shape since the shape parameters were very different, but there sizes are roughly the same.

9 Recommendation

The micro-CT scans can be used to select best candidates among the eggs for thin sectioning and determining the position and the orientation for the plane of thin sectioning that will optimize variety of the thin sections and facilitate interpretation. The metal residues inside the egg cavities, the metal seepage between the half shell and the wrapping layer or the material surrounding the vesicles as well as the glassy and non-glassy layers on the external egg surface could be targeted. Most of the XRF data was only collected on the outside of the eggs and are semi-quantitative and incomplete.

Further research should also be done on the iron object, which seemed to look like a metal tool. The object was found to fit tightly in only a few crucibles and was therefore not used to shape systematically all the egg cavities. The tool was also found to be too small to fit around the crucibles and was therefore not used as some kind of grip tool. Careful and cleaning of the tool after impregnation of the iron crust can precise the shape and use this object. The tool was found with the crucibles. However, it might not have been used to produce them and was to be molten.

Digital models of negatives of imprints with size information and 3D prints should be produced and circulated among community of Western Europe archaeologists specialised in metal usage in the Middle Iron Age to facilitate object identification.

For the calculations of the breadth, width and length of the eggs, Avizo 9.3 have been used. Avizo 9.3 states that the 3D feret measures rely on sampling in a distribution of different directions (31 directions by default). When increasing this number of directions to 62, it turned out the width changed by roughly 2mm. When increasing even more, the width did not change any further. Therefore calculations of the width should be redone for a more accurate result.

Bibliography

1 Transect (2016). Evaluatierapport Archeologische Begeleiding (protocol Proefsleuven) Sportcomplex Spoordijk, Gemeente Tilburg, *Onderzoeksmeldingscode: 3295861100.* Not yet published. 19 p.

2 Ngan-Tillard D.J.M. and Huisman, D.J. (2017). Micro-CT Scanning. Chapter 42, Archaeological Soil and Sediment Micromorphology, Cristiano Nicosia & Georges Stoops (eds), Wiley, 496 p.

3 Tarplee, M.F.V., van der Meer, J.J.M. & Davis, G.R. (2011) The 3D microscopic 'signature' of strain within glacial sediments revealed using X-ray computed microtomography. Quaternary Science Reviews 30, 3501–3532.

4 https://nl.wikipedia.org/wiki/R%C3%B6ntgenfluorescentie

Personal communications

5 Huisman, pers. communication, 2017. E-mail and We-transfer to d.j.m.ngan-tillard@tudelft.nl dated 03-03-2017

6 Ngan-Tillard, oral communications, summer 2017.

7 Van Os, pers. communication 2017 E-mail to alicia_bach@hotmail.com dated xx

8 Wolf, pers. communication 2017, oral communication with Ngan-Tillard, 04-2017.

Appendix I: Micro-CT images of eggs

In this appendix the images of all crucibles that have been made with Avizo 9.3 can be found.

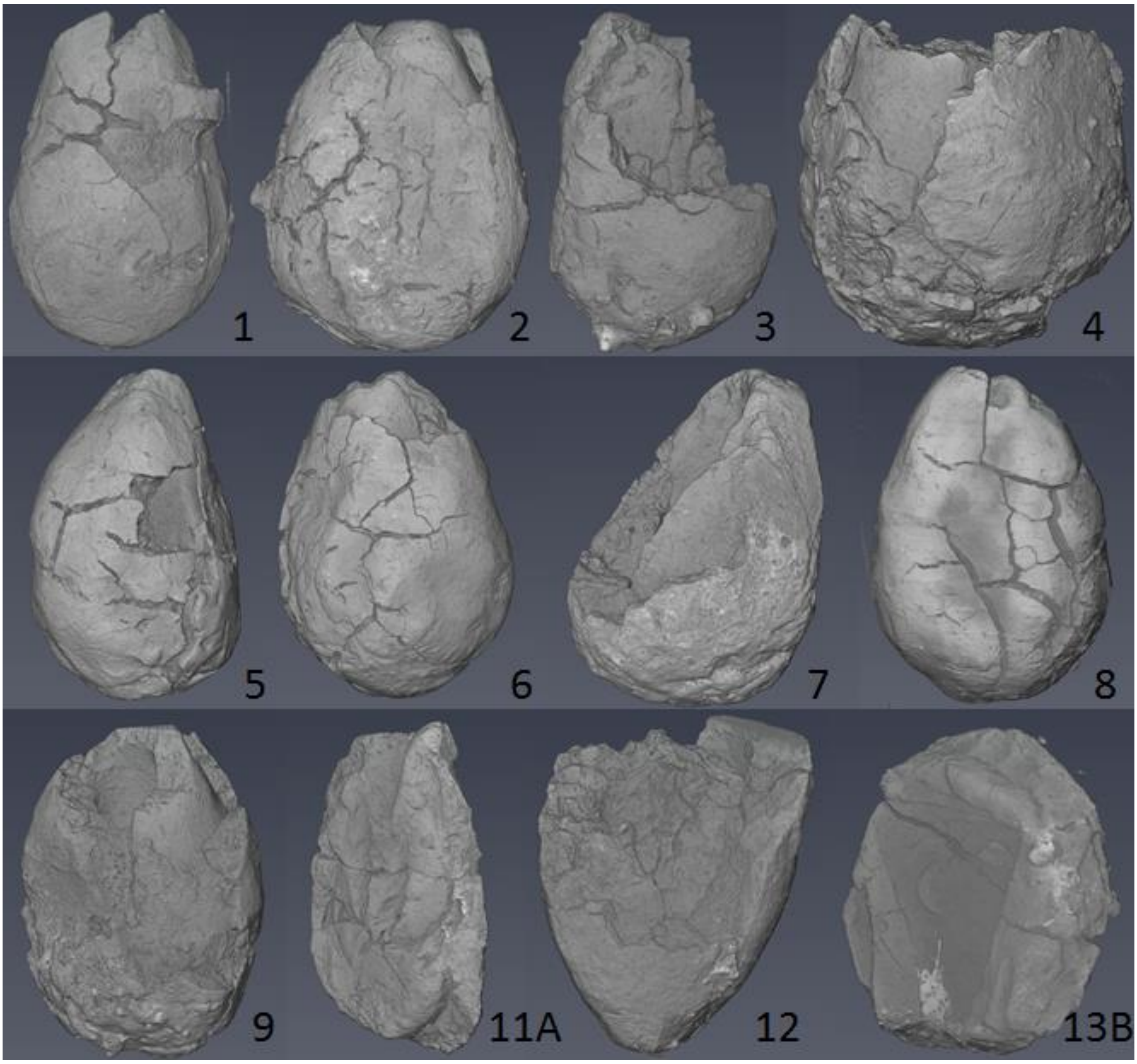

Figure 23 Images of all crucibles

Appendix II: XRF Results

In this appendix the results of the XRF scanning produced by Bertil van Os[6] can be found.

xrfnummer	vondstnum	opgraving	Time	Duration	Type	SiO2	CaO	P2O5	K2O	Al2O3	TiO2	Fe2O3	MnO	Bal
						%	%	%	%	%	%	%	%	%
Scan numr	Egg	Place on egg												
760	1	Glacy part	12-05-17 10:31	110	Mining	70	5.03	0.715	6.08	3.18	0.363	2.35	0.205	12
761	1	Red spots	12-05-17 10:34	110	Mining	57	0.153	0.351	1.05	4.51	0.712	3.46	0.056	32
762	1	Big point	12-05-17 10:37	110	Mining	35	0.187	~~0.451~~	0.986	2.82	0.555	5.07	0.083	55
763	1	Background (less glacy part)	12-05-17 10:41	110	Mining	52	1.17	0.881	2.29	5.41	0.662	2.85	0.124	34
764	1	Inside part	12-05-17 10:44	110	Mining	15	0.134	0.680	0.820	5.74	0.631	4.16	0.036	73
765	2	Little spot	12-05-17 10:49	110	Mining	60	1.28	0.491	3.11	3.46	0.464	7.17	0.120	24
766	2	Red spots	12-05-17 10:53	110	Mining	59	2.06	0.431	3.98	2.60	0.499	2.47	0.094	29
767	2	Yellow part	12-05-17 10:57	110	Mining	57	5.44	1.26	3.74	2.77	0.576	2.38	0.286	26
768	2	Inside part	12-05-17 11:05	110	Mining	50	0.360	1.18	1.18	7.66	0.859	3.39	0.047	35
769	3	Bubble (3-1)	12-05-17 11:09	110	Mining	40	2.35	1.94	2.89	3.89	0.336	24	0.278	24
770	3	Black part	12-05-17 11:14	110	Mining	52	3.55	0.885	3.15	2.39	0.269	6.59	0.263	31
771	3	Black part (2)	12-05-17 11:17	110	Mining	51	4.05	0.875	3.25	2.79	0.402	5.57	0.213	32
772	3	Green part	12-05-17 11:21	110	Mining	67	5.40	0.395	5.94	0.987	0.382	1.60	0.248	18
773	3	Zwarte 'korrel'	12-05-17 11:23	110	Mining	20	1.08	0.522	1.41	2.25	0.275	28	0.126	46
774	3	Green part in the middle	12-05-17 11:28	110	Mining	58	7.56	0.341	4.61	0.682	0.238	1.43	0.061	27
778	7	Green part on the bottom	12-05-17 12:29	110	Mining	64	3.83	0.380	5.37	1.83	0.402	2.15	0.329	21
779	7	Black spot	12-05-17 12:32	110	Mining	68	2.99	0.350	4.84	2.82	0.463	2.08	0.338	18
781	7	Inside part	12-05-17 12:38	110	Mining	38	0.114	1.04	0.957	6.08	0.756	3.61	~~0.018~~	49
782	7	Inside part	12-05-17 12:41	110	Mining	29	0.104	0.217	0.824	1.40	0.643	4.10	~~0.023~~	64
783	9	Red spots	12-05-17 12:46	110	Mining	53	3.72	0.495	4.27	1.61	0.361	4.39	0.157	32
784	9	Red spots	12-05-17 12:50	110	Mining	59	2.14	0.288	5.18	1.93	0.390	2.07	0.070	29
785	9	Spot on the bottom	12-05-17 12:53	110	Mining	59	3.54	0.575	3.05	3.81	0.510	2.38	0.182	27
786	11	White spot	12-05-17 12:58	110	Mining	23	0.156	1.66	1.01	4.74	0.585	3.08	0.028	66
787	11	See image 11A-1	12-05-17 13:01	110	Mining	44	3.35	0.447	3.69	2.67	0.377	2.84	0.179	43
788	11	See image 11A-2	12-05-17 13:04	110	Mining	43	3.41	0.361	3.35	2.97	0.432	3.37	0.160	43
789	12	Black spot	12-05-17 13:10	110	Mining	17	1.55	0.694	2.43	1.55	0.287	19	0.206	58
790	13	White 'korrel' + red spots	12-05-17 13:15	110	Mining	40	1.28	0.457	3.34	0.864	0.437	3.49	0.131	50
791	13	Black part	12-05-17 13:20	110	Mining	47	5.72	0.873	6.76	0.843	0.254	13	0.690	25
792	13	Black bubble on the back	12-05-17 13:24	110	Mining	31	0.889	0.807	2.40	2.83	0.617	30	0.142	32

S	Cl	Mg	Zn	Cu	Co	Sn	Pb	Cr	Zr	Sr	Rb	As
%	mg/kg	mg/kg	mg/kg	mg/kg	mg/kg	mg/kg	mg/kg	mg/kg	mg/kg	mg/kg	mg/kg	mg/kg
0.048	~~63~~	11114	17	263	~~86~~	~~23~~	~~6.66~~	~~85~~	457	230	320	~~6.83~~
0.089	~~48~~	~~5329~~	49	128	~~97~~	28	~~9.21~~	148	526	63	91	9.74
0.047	~~50~~	~~5114~~	95	139	~~124~~	38	26	116	595	75	153	12
0.208	~~52~~	~~6316~~	20	217	~~89~~	~~31~~	~~7.87~~	228	524	82	172	7.01
0.289	~~59~~	~~6456~~	69	326	~~108~~	42	24	153	411	58	149	15
0.107	~~52~~	7958	46	1107	~~151~~	43	~~8.88~~	144	507	86	195	8.63
0.095	~~63~~	~~10615~~	34	778	~~89~~	25	~~8.24~~	133	521	89	199	11
0.102	~~65~~	~~13962~~	102	1289	~~90~~	56	8.90	92	527	338	221	8.53
0.268	~~53~~	6806	60	282	~~96~~	37	19	125	495	68	146	7.05
0.117	~~61~~	~~12271~~	49	886	284	49	~~11~~	257	444	319	264	74
0.095	~~63~~	~~14233~~	21	386	~~133~~	~~41~~	~~7.31~~	118	478	275	260	7.89
0.083	~~68~~	~~9556~~	19	479	~~128~~	~~32~~	~~7.39~~	~~143~~	435	213	220	6.44
0.055	~~82~~	~~11600~~	~~17~~	199	~~78~~	~~39~~	~~6.90~~	120	518	301	373	~~8.41~~
0.079	205	~~11457~~	24	407	~~269~~	~~49~~	~~11~~	296	435	101	160	30
0.035	~~78~~	~~11384~~	~~17~~	103	~~92~~	~~25~~	~~11~~	~~67~~	415	181	285	~~5.36~~
0.031	~~67~~	~~9388~~	~~18~~	51	~~87~~	~~24~~	~~6.89~~	90	494	191	258	~~5.30~~
0.047	~~64~~	~~8930~~	~~16~~	70	~~88~~	~~34~~	~~6.93~~	~~88~~	465	176	245	~~5.86~~
0.263	~~59~~	~~5717~~	25	110	~~106~~	26	~~6.71~~	102	489	65	151	15
0.049	~~78~~	~~7070~~	52	238	~~137~~	~~32~~	~~13~~	138	539	69	129	10
0.058	~~63~~	~~9026~~	~~17~~	600	~~110~~	46	~~7.12~~	85	453	150	243	~~5.96~~
0.073	~~59~~	8843	~~18~~	1988	~~81~~	134	~~6.46~~	98	461	89	207	8.44
0.066	~~59~~	12707	~~16~~	179	~~85~~	29	~~7.92~~	96	449	192	269	~~5.17~~
0.259	~~54~~	~~7675~~	217	2355	~~103~~	2593	341	135	416	62	141	90
0.098	~~55~~	7831	50	204	~~92~~	32	11	97	542	162	300	9.88
0.098	~~61~~	~~12002~~	27	316	~~106~~	32	~~8.58~~	~~75~~	506	169	279	8.02
0.084	122	10972	45	318	~~206~~	~~31~~	~~8.76~~	288	383	121	172	20
0.082	~~58~~	7323	91	1393	~~110~~	345	79	120	491	108	259	18
0.046	~~72~~	~~13760~~	~~21~~	705	~~209~~	47	~~9.57~~	268	482	306	458	18
0.078	190	~~18915~~	47	324	~~292~~	~~38~~	~~12~~	411	380	79	217	36

Ba	V	Ag	Ni	Sb	Cd	Mo	Nb	Au	Se	W	Bi	Pd
mg/kg	mg/kg	mg/kg	mg/kg	mg/kg	mg/kg	mg/kg	mg/kg	mg/kg	mg/kg	mg/kg	mg/kg	mg/kg
384	~~89~~	~~37~~	~~42~~	~~18~~	~~8.98~~	~~2.01~~	17	~~9.04~~	~~2.34~~	~~52~~	11	~~4.47~~
279	~~53~~	~~34~~	~~40~~	~~17~~	~~8.70~~	~~2.03~~	20	~~8.99~~	~~2.14~~	~~50~~	11	~~4.36~~
284	54	~~38~~	~~47~~	~~20~~	~~10~~	~~2.45~~	21	~~10~~	~~2.76~~	~~57~~	19	~~5.03~~
300	~~51~~	~~31~~	~~41~~	~~17~~	~~8.94~~	~~2.06~~	20	~~9.33~~	~~2.17~~	~~52~~	14	~~4.51~~
307	~~85~~	~~33~~	~~43~~	~~19~~	~~9.55~~	~~2.10~~	16	~~9.37~~	~~2.65~~	~~54~~	14	~~4.84~~
422	~~55~~	~~60~~	~~46~~	~~19~~	~~9.75~~	~~2.30~~	20	~~10~~	~~2.64~~	~~62~~	14	~~4.76~~
347	~~49~~	~~36~~	~~43~~	~~18~~	~~9.03~~	~~2.18~~	19	~~9.39~~	~~2.46~~	~~67~~	11	~~4.56~~
497	~~90~~	~~52~~	~~45~~	~~18~~	~~9.36~~	~~2.30~~	19	~~9.83~~	~~2.57~~	~~88~~	11	~~4.69~~
265	~~55~~	~~41~~	~~41~~	~~17~~	~~8.86~~	~~1.97~~	18	~~8.99~~	~~2.21~~	~~70~~	10	~~4.37~~
1020	~~84~~	~~163~~	68	~~28~~	~~14~~	~~3.41~~	12	~~19~~	~~4.32~~	~~81~~	~~9.38~~	~~7.24~~
484	~~77~~	~~75~~	~~44~~	~~20~~	~~10~~	~~2.23~~	12	~~10~~	~~2.59~~	~~54~~	8.90	~~5.08~~
483	~~71~~	~~67~~	~~56~~	~~20~~	~~10~~	~~2.25~~	9.92	~~10~~	~~2.45~~	~~57~~	~~7.92~~	~~5.21~~
335	~~68~~	~~24~~	~~42~~	~~19~~	~~9.90~~	~~2.28~~	15	~~9.45~~	~~2.49~~	~~53~~	~~8.29~~	~~4.87~~
546	~~72~~	~~100~~	137	~~27~~	~~13~~	~~3.38~~	14	~~14~~	~~5.20~~	~~90~~	~~7.89~~	~~6.77~~
354	~~32~~	~~37~~	~~42~~	~~24~~	~~9.54~~	~~2.05~~	14	~~9.22~~	~~2.53~~	~~52~~	~~7.74~~	~~4.66~~
330	~~87~~	~~24~~	~~43~~	~~19~~	~~9.68~~	~~2.20~~	15	~~9.30~~	~~2.49~~	~~52~~	~~7.82~~	~~4.67~~
322	~~53~~	~~24~~	~~44~~	~~19~~	~~9.81~~	~~2.27~~	17	~~9.94~~	~~2.61~~	~~55~~	~~7.91~~	~~4.88~~
104	~~53~~	~~30~~	~~43~~	~~28~~	~~15~~	~~2.34~~	19	~~9.09~~	~~2.25~~	~~55~~	11	~~7.02~~
193	~~79~~	~~40~~	~~55~~	~~36~~	~~15~~	~~3.21~~	19	~~13~~	~~3.67~~	~~77~~	16	~~7.87~~
351	~~45~~	~~41~~	~~43~~	~~18~~	~~9.51~~	~~2.14~~	16	~~9.34~~	~~2.42~~	~~51~~	~~7.62~~	~~4.79~~
321	~~39~~	~~41~~	~~42~~	~~19~~	~~9.42~~	~~2.10~~	16	~~9.10~~	~~2.17~~	~~51~~	14	~~4.50~~
400	48	~~55~~	~~42~~	~~18~~	~~8.79~~	~~2.00~~	16	~~9.26~~	~~2.23~~	~~50~~	13	~~4.62~~
254	48	~~25~~	~~47~~	~~20~~	~~12~~	~~2.30~~	16	~~11~~	~~2.75~~	~~62~~	11	~~5.04~~
302	49	~~32~~	~~41~~	~~21~~	~~9.08~~	~~2.16~~	19	~~9.25~~	~~2.29~~	~~50~~	14	~~4.39~~
284	~~42~~	~~23~~	~~44~~	~~19~~	~~10~~	~~2.36~~	19	~~9.89~~	~~2.64~~	~~56~~	~~12~~	~~5.12~~
461	~~134~~	~~75~~	84	~~24~~	~~12~~	~~2.55~~	7.76	~~12~~	~~3.31~~	~~63~~	~~7.19~~	~~5.80~~
383	~~40~~	~~49~~	~~47~~	~~20~~	~~11~~	~~2.43~~	18	~~11~~	~~2.81~~	~~60~~	~~8.86~~	~~5.12~~
972	~~141~~	~~55~~	~~88~~	~~26~~	~~13~~	~~3.13~~	10	~~13~~	~~3.71~~	~~101~~	~~9.82~~	~~6.78~~
755	110	~~174~~	152	~~29~~	~~15~~	~~5.29~~	13	~~15~~	~~4.67~~	~~112~~	~~9.51~~	~~7.27~~